Electroexcitation of ^{6}Li with application to the reactions ^{6}Li$(\pi^-,\gamma)_{1s}$ ^{6}He$(0^+,2^+)$

J. C. Bergstrom
Saskatchewan Accelerator Laboratory, University of Saskatchewan, Saskatoon S7N 0W0, Canada
(Received 5 September 1979)

The transverse form factor for the 5.37 MeV($2^+,T=1$) level of ^{6}Li is analyzed in terms of a phenomenological model to give the configuration amplitudes and transition density. Radiative pion capture rates for the 1s atomic orbital of ^{6}Li leading to the two lowest states of ^{6}He are estimated using the phenomenological functions. The radiative pion capture rate to ^{6}He(g.s.) agrees with experiment, but the rate to ^{6}He(2^+,1.8 MeV) is larger than the measured value. It is shown that if the longitudinal form factor is small at $q \approx m_\pi$, the transverse 5.37 MeV form factor gives the radiative pion capture matrix elements directly. As part of this study, the $C2$ form factor was measured near $q = m_\pi$, and its implications on the wave functions are considered.

[NUCLEAR REACTIONS ^{6}Li(e,e'), E=76–141 MeV; $\sigma(E;E_{e'},\theta)$. ^{6}Li deduced form factors, wave functions, radiative capture.]

I. INTRODUCTION

In a recent paper, Renker *et al.*[1] presented measurements of the radiative pion capture (RPC) rate from the 1s atomic orbital in ^{6}Li leading to the ground and first excited states of ^{6}He. By eliminating the contribution from the competitive p-state capture, interpretation of the results becomes greatly simplified. For example, the 1s capture rate in the impulse approximation (neglecting nucleon Fermi motion) is primarily determined by the nuclear matrix element of $\tau^-\vec{\sigma}\cdot\vec{\epsilon}_\lambda e^{-i\vec{k}\cdot\vec{r}}$ between ^{6}Li and ^{6}He. This operator is related by isospin rotation to the spin-dependent part of the (e,e') interaction leading to the corresponding analog state in ^{6}Li. In other words, the same nuclear matrix elements occur in 1s radiative capture and electron scattering when the final states belong to the same isospin multiplet.

In this work, we use the information provided by the electron scattering form factors for the 3.56 MeV ($0^+,T=1$) and 5.37 MeV ($2^+,T=1$) levels of ^{6}Li to estimate the $(\pi^-,\gamma)_{1s}$ rates to the ground ($0^+,T=1$) and 1.80 MeV ($2^+,T=1$) states of ^{6}He. The transition to the 2^+ state is complicated by the fact that the transverse form factor for the 5.37 MeV state does not have a unique multipolarity, but can in principle be a mixture of $M1$, $E2$, and $M3$ components. Therefore, we have performed a phenomenological analysis of this form factor similar to that previously done for the 3.56 MeV $M1$ transition.[2,3] From this, we conclude that electroexcitation of the 5.37 MeV level is predominantly $E2+M3$ in character, with nearly equal contributions from each multipole.

For excitations involving recoupling within a $(1p)^n$ configuration, we show that the convection current matrix element vanishes for $M3$ transitions, and is negligible for $E2$ transitions providing the longitudinal ($C2$) form factor is small. Then only the spin-dependent magnetization density contributes, and the $(\pi^-,\gamma)_{1s}$ nuclear matrix elements may be obtained directly from the corresponding $E2$ or $M3$ form factors, assuming the simple impulse approximation is valid.

We have measured the longitudinal form factor of the 5.37 MeV state near the momentum transfer appropriate for the radiative capture reaction and verified that it is small. The capture rate to ^{6}He(2^+) derived directly from the 5.37 MeV transverse form factor is shown to be in reasonable agreement with the result derived from the phenomenological functions.

The 1s capture rate to ^{6}He(g.s.) is found to be in good agreement with the measurement of Renker *et al.*, but the transition to ^{6}He(2^+) is two standard deviations above the experimental value. On the other hand, our estimate of the ratio of the (γ,π^+) cross sections to the same states is in accord with the result of Audit *et al.*[4]

II. MEASUREMENT OF $F_L^2(q)$ FOR THE 5.37 MeV LEVEL

As alluded to in the Introduction, the longitudinal form factor of the 5.37 MeV level provides a measure of the convection current contribution to the transverse $E2$ form factor, and also provides a constraint on the phenomenological wave functions. In this section, we briefly discuss the present measurement of this form factor. Unfortunately, because of the natural width of this state ($\Gamma_{tot} \approx 0.55$ MeV), and its disposition relative to the much larger and broader 4.31 MeV ($2^+,T=0$) level,

even a crude measurement is extremely difficult and time consuming. Furthermore, the 5.37 MeV total form factor is known to be predominantly transverse in character,[5,6] so the longitudinal contribution is small even at forward electron scattering angles.

This measurement was made at the electron scattering facility of the Saskatchewan accelerator laboratory. The target was 99% isotopically enriched ^{6}Li metal rolled to a thickness of about 20 mg/cm^2. Incident beam currents were kept below 2.5 μA to avoid target melting. The total momentum resolution, as given by the elastic peak full-width at half maximum (FWHM), was about 0.15%.

The longitudinal and transverse form factors are related to the differential cross section by

$$\sigma_M^{-1}\frac{d\sigma}{d\Omega}=F_L^2(q)+\left(\frac{1}{2}+\tan^2\frac{\theta}{2}\right)F_T^2(q)$$
$$=F_{\text{tot}}^2(q,\theta), \quad (1)$$

where σ_M is the Mott cross section for a point charge Ze. The form factors were separated in the usual way by measuring the angular dependence of $F_{\text{tot}}^2(q,\theta)$ at a fixed momentum transfer q. In this experiment, the scattering angles and associated incident energies were 59.0° (140.9 MeV), 90.0° (99.3 MeV), and 140.0° (75.6 MeV), corresponding to $q=0.687$ fm^{-1}.

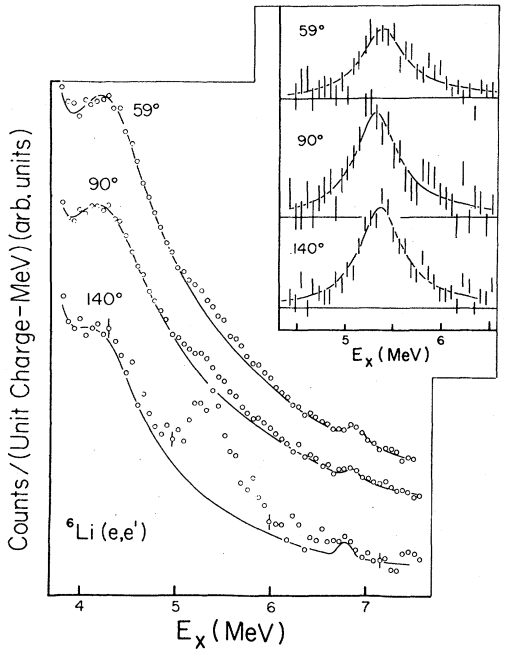

FIG. 1. Electron scattering spectra from ^{6}Li showing the 5.37 MeV peak on the flank of the broad 4.31 MeV (2^+) resonance. The three spectra do not have a common scale factor. The solid curve represents the total background under the 5.37 MeV resonance and the inset shows the background-subtracted spectra. The Breit-Wigner curves were fit simultaneously with the background by a least-squares procedure. The small peak near 7 MeV is the 7.66 MeV (0^+) state of ^{12}C, apparently introduced during target fabrication.

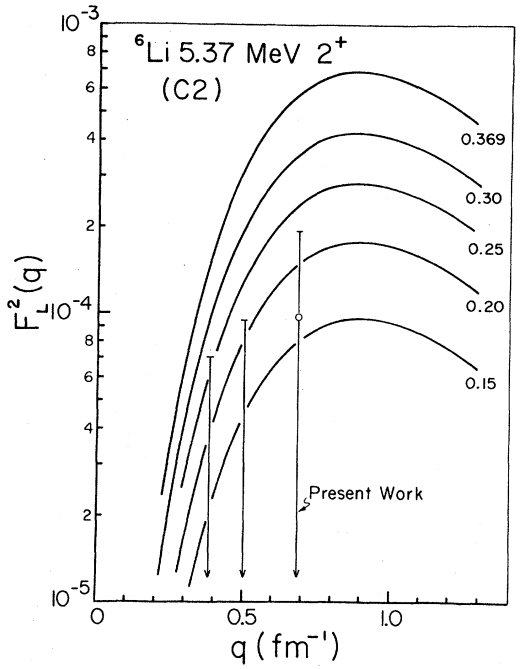

FIG. 2. Longitudinal form factors of the 5.37 MeV state based on the phenomenological densities and amplitudes determined from the experimental transverse form factor. The curves are labeled by β, the ground state $^1P_1$ amplitude. The experimental result at $q=0.69$ fm^{-1} is from the present work, the others are from Ref. 5.

The area of the 5.37 MeV peak was determined by simultaneously fitting the (e,e') spectra with a series of shape functions describing the inelastic peaks, plus a polynomial representing the elastic peak radiation tail and the various breakup continua.[3] Breit-Wigner resonances were used for the 4.31 and 5.37 MeV peaks. The position of the 5.37 MeV shape function, having been determined from the back-angle data (and previous work), was not allowed to vary during the fitting procedure, and its total natural width was fixed at $\Gamma_{\text{tot}}=0.55$ MeV.

The line-shape fits in the region of the 5.37 MeV state are illustrated in Fig. 1, where the curves represent the total "background" under the resonance. When these are subtracted from the data, we obtain the spectra shown in the inset. The Breit-Wigner curves in this figure describe the fits to the 5.37 MeV peak generated during the least-squares spectrum analysis.

The area of the 5.37 MeV peak was normalized

TABLE I. Summary of the present experimental results for the 5.37 MeV ($2^+, T=1$) state of ^{6}Li. Radiative corrections and the elastic form factor were calculated as in Ref. 3. The total form factor is defined within ±0.55 MeV of the peak center. Errors do not reflect uncertainties in the position and width of the state.

E_0 (MeV)	θ (deg)	$\sigma(5.37)/\sigma(\text{el})$ ($\times 10^3$)	$F_{\text{el}}^2(q)$ (calc.)	$F_{\text{tot}}^2(q,\theta)$ ($\times 10^4$)
140.9	59.0	1.12 ± 0.20	0.364	4.08 ± 0.71
99.3	90.0	1.80 ± 0.32	0.358	6.43 ± 1.14
75.6	140.0	8.83 ± 0.79	0.352	31.1 ± 2.8

$q = 0.687$ fm^{-1}
$F_L^2(q) = (9.7 \pm 9.5) \times 10^{-5}$
$F_T^2(q) = (3.73 \pm 0.40) \times 10^{-4}$

to the elastic peak, which in turn was evaluated by phase shift analysis, and radiative corrections were made as discussed elsewhere.[3] The results are summarized in Table I, and as before, the form factor represents the strength within $\pm\Gamma_{\text{tot}}$ of the peak maximum. From a least-squares fit of $F_{\text{tot}}^2(q,\theta)$ vs $\frac{1}{2}+\tan^2\theta/2$, we obtain the separate form factors given in Table I. The present and previous[5] measurements of $F_L^2(q)$ are displayed in Fig. 2.

III. PHENOMENOLOGICAL ANALYSIS OF THE 5.37 MeV FORM FACTOR

Our purpose here is twofold. First, we require wave functions and transition densities to estimate the $(\pi^-,\gamma)_{1s}$ matrix elements. Second, we must establish the $M1$ contribution to the 5.37 MeV transverse form factor, since if it is large, one cannot expect the $(\pi^-,\gamma)_{1s}$ estimate based directly on the form factor to be reliable (the $M1$ form factor need not have a negligible convection current part).

We assume a $(1p)^2$ model space and L-S wave functions

$$\Psi_{\text{gnd}}(1^+,0) = \alpha\,{}^3S_1 + \beta{}^1P_1 + \gamma{}^3D_1\,, \tag{2}$$

$$\Psi_{5.37}(2^+,1) = G{}^3P_2 + H{}^1D_2\,, \tag{3}$$

where[2,7]

$$\alpha = 0.924, \quad \beta = 0.369, \quad \gamma = 0.102\,. \tag{4}$$

The inelastic transverse form factor in general contains $M1$, $E2$, and $M3$ terms,

$$F_T^2(q) = F_{M1}^2(q) + F_{E2}^2(q) + F_{M3}^2(q)\,, \tag{5}$$

where the individual form factors are given by

$$F_{M1}(q) = \left(\frac{q}{m}\right)[C_0\langle j_0(qr)\rangle + C_2\langle j_2(qr)\rangle] f_p f_{\text{c.m.}}\,, \tag{6}$$

$$F_{E2}(q) = \mu_v D\left(\frac{q}{m}\right)\langle j_2(qr)\rangle f_p f_{\text{c.m.}}\,, \tag{7}$$

$$F_{M3}(q) = \mu_v E\left(\frac{q}{m}\right)\langle j_2(qr)\rangle f_p f_{\text{c.m.}}\,. \tag{8}$$

Here $\mu_v = \mu_p - \mu_n = 4.706$, m is the nucleon mass, and the coefficients C_0, C_2, D, and E are functions only of the ground and excited state amplitudes. The proton and center of mass form factors, f_p and $f_{\text{c.m.}}$, and the radial matrix elements $\langle j_\lambda(qr)\rangle$ are defined in Ref. 3. As before, the radial density is expanded in a convenient series, with coefficients to be determined by the experimental data. The only difference from the procedure described in Ref. 3 is that here we do not assume the radial density $[R'(r)R(r)]$ is normalized to unity. The 5.37 MeV level is unbound to two- and three-body breakup, so the radial wave function $R'(r)$ may be more spread out than the ground state function $R(r)$.

Most of the experimental results were obtained using Breit-Wigner fits to the spectra, and $F_T^2(q)$ is defined within $\pm\Gamma_{\text{tot}}$ of the peak center. Consequently, the theoretical form factors must be renormalized downward to account for the strength not included within this limit[3]

$$[F^2(q)]_{\text{exp}} = [F^2(q)]_{\text{theor}}/1.42\,. \tag{9}$$

The transverse form factor expressed by Eqs. (5)–(8) was fitted by the method of least squares to 37 data points from Refs. 3,5,8, some unpublished Saskatoon results, and the present measurement. No corrections were made for Coulomb distortion effects, which are usually small for very light nuclei. Most of the data were obtained at large scattering angles, and in view of the upper limits on $F_L^2(q)$, are essentially transverse in character. With the ground state configuration given by Eq. (4), the fitting procedure was repeated for various excited state amplitudes (G,H) until a minimum in the chi-square per degree of freedom, χ_ν^2, was located. One finds two solutions for the 5.37 MeV amplitudes (G,H) which give comparable χ_ν^2, represented by $G>0$ and $G<0$, where H is considered positive. The $G<0$ solution is rejected for reasons discussed later.

When the wave functions and radial density which give the best fit are used to evaluate the longitudinal form factor, given by

$$F_L(q) = (1/\sqrt{6})[(\tfrac{9}{60})^{1/2}G\gamma - H\beta]\langle j_2(qr)\rangle f_p f_{\text{c.m.}}\,, \tag{10}$$

we obtain the curve in Fig. 2 labeled $\beta = 0.369$, the ground state $^1P_1$ amplitude. Although the experimental errors are large, the discrepancy with theory is evident. The source does not likely lie in the amplitudes (G,H), since the transverse form

factor is mainly determined by the product αH, and $\alpha \approx 0.9$–1.0 for most theories of ^{6}Li. We must therefore consider the possibility that β as given in Eq. (4) is too large.

In order to find a range of β values consistent with the transverse and longitudinal form factors, the fitting procedure was repeated for a series of ground state amplitudes. For a given β, the amplitudes α and γ were constrained by the quadrupole moment[2] using a $1p$-shell rms radius $\langle r^2\rangle_p^{1/2} = 3.46$ fm (Ref. 3) (the magnetic moment is somewhat less sensitive to the amplitudes). The predicted longitudinal form factors, as a function of β, are summarized in Fig. 2.

Inspection of Fig. 2 suggests $\beta \lesssim 0.20$. However, since the ground state magnetic moment deviates monotonically from the experimental value for $\beta < 0.369$, as a compromise we will adopt $\beta = 0.200$ as our alternative estimate of this amplitude. The respective magnetic moment is 5% above the experimental value, not an unreasonable difference considering we have ignored configurations higher than $(1p)^2$, as well as two-body contributions. Both sets of amplitudes are presented in Table II

The normalization of the radial density $[R'R]$, also determined by the least-squares fit, is slightly less than unity. The transition radius, defined as the rms radius of $[R'R]$, is estimated to be $\langle r_t^2\rangle^{1/2} = 3.78$ fm.

The 5.37 MeV transition density parameters (b, a_n) for $\beta = 0.200$ and $G = 0.460$ are as follows:

$$b = 2.324 \text{ fm}, \quad a_2 = 6.641 \times 10^{-2} \text{ fm}^{-5}$$

$$a_3 = -3.502 \times 10^{-2} \text{ fm}^{-6}, \quad a_4 = 7.427 \times 10^{-3} \text{ fm}^{-7}$$

$$a_6 = -1.668 \times 10^{-4} \text{ fm}^{-9}, \quad a_8 = 2.619 \times 10^{-6} \text{ fm}^{-11}. \quad (11)$$

Since the χ_ν^2 and corresponding (G, H) are nearly independent of b, we have arbitrarily used the value obtained from the 3.56 MeV form factor analysis.[3] According to Eq. (9) the a_n must be multiplied by $(1.42)^{1/2}$ to represent the entire resonance.

The fit to the transverse form factor with the $\beta = 0.200$ amplitudes of Table II is shown in Fig. 3, along with its multipole components. The $E2$ and $M3$ contributions are nearly equal, but the $M1$ form factor is suppressed and has a diffraction minimum at $q = 0.75$ fm^{-1}. Actually, the multipole form factors do not change significantly between the two sets of amplitudes, suggesting the decomposition shown in Fig. 3 is not strongly model dependent.

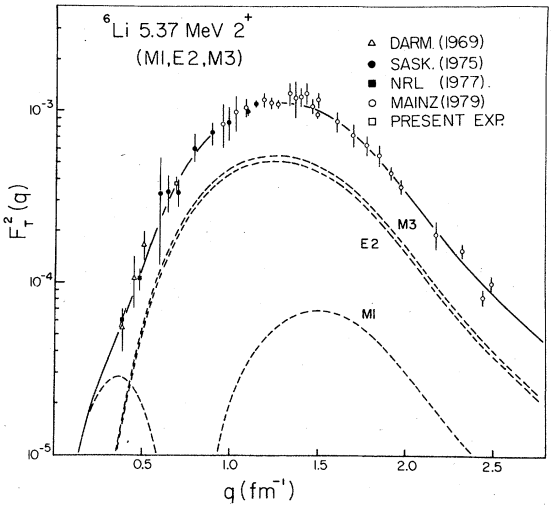

FIG. 3. Transverse form factor of the 5.37 MeV state and its multipole components compared with the data. The curves represent the least-squares fit with the $\beta = 0.200$ amplitudes of Table II. The $E2$ and $M3$ form factors have the same q dependence [see Eqs. (7) and (8)], differing only in their normalization. The peculiar change in slope of the fit above $q = 2$ fm^{-1} is caused by the absence of any constraints on the physical form factor at high momentum transfers, and should not be considered as realistic.

The $M1$ form factor gives the ground state $M1$ radiative width for the entire 5.37 MeV resonance:

$$\Gamma_{\gamma 0}(M1) = 0.27 \pm 0.05 \text{ eV}. \quad (12)$$

Finally, for completeness, we make a few re-

TABLE II. Configuration amplitudes for the ground state and excited $T = 1$ states of ^{6}Li as obtained from the phenomenological analyses. The set labeled C is preferred if the 5.37 MeV $C2$ form factor is considered an acceptable constraint. The L–S wave functions are defined by Eqs. (2), (3), and (13).

Ground $(1^+, T=0)$			5.37 MeV $(2^+, T=1)$		3.56 MeV $(0^+, T=1)$		
α	β	γ	G	H	A	B	
0.979	0.200	0.041	0.460	0.888	0.881 ± 0.018	-0.473 ± 0.034	(C)
					0.996 ± 0.004	0.087 ∓ 0.039	(D)
0.924	0.369	0.102	0.360	0.933	0.843 ± 0.022	-0.537 ± 0.034	(A)
					1.00	-0.012 ± 0.041	(B)

marks about the 3.56 MeV $M1$ form factor. The L-S wave function for the 3.56 MeV $(0^+, T=1)$ state in a $(1p)^2$ configuration space is

$$\Psi_{3.56}(0^+,1)=A^1S_0+B^3P_0\,. \tag{13}$$

Previous analyses of this form factor utilized the wave functions corresponding to $\beta=0.369$. Since the present work suggests the $\beta=0.20$ ground state may be more realistic, we have reanalyzed this transition and give an alternative set of excited state amplitudes which we call sets C and D, to distinguish them from the former A and B solutions (Table II). As before, we use the ground state radiative width as a constraint, and the amplitude uncertainties reflect the experimental error on this quantity.

The new amplitudes yield a transition density virtually indistinguishable from that of Ref. 3. The β-decay $ft_{1/2}$ value for ^{6}He, and the threshold photopion cross section leading to ^{6}He(g.s.) have been recalculated with the C amplitudes in Table II. With the coupling constants employed by Cammarata and Donnelly,[7] we obtain $ft_{1/2}=789\pm23$, compared with the "experimental" value $f_{1/2}=814$ (Ref. 9). The photopion cross section is $7\pm4\%$ higher than our previous estimate.[2]

IV. COMPARISON OF PHENOMENOLOGICAL AND THEORETICAL AMPLITUDES

Since the phenomenological amplitudes were generated by fitting various electromagnetic form factors with no consideration given to the nuclear potentials, residual interactions, etc., it is worthwhile comparing the present results with the amplitudes derived from more fundamental approaches. Here, we consider two examples.

The first example is obtained by diagonalizing the Hamiltonian matrix using the Kuo-Brown two-body matrix elements in a $(1p)^2$ model space. The single-particle energy difference $\epsilon=E(1p_{1/2})-E(1p_{3/2})$ is probably somewhere around 3–5 MeV for ^{6}Li, and indeed as shown in Table III, the theoretical and phenomenological amplitudes of the ground and 5.37 MeV states compare favorably for $\epsilon=3$–4 MeV. The situation with the 3.56 MeV state is not so favorable, the shell model giving a smaller $L=1$ component than the phenomenological analysis. Although the predicted 2^+-0^+ separation is 1.76 MeV, in good agreement with experiment, the excitation energies relative to the ground state are about 1.8 MeV too low.

For the second example, we consider the calculation by Barker[10] which relies on the known excitation energies to determine the exchange mixture in the effective shell model interaction. The resulting amplitudes are given in Table III.

Both calculations give wave functions that are more or less consistent with the phenomenological results. Note that the theoretical values of G are positive, which is the principal reason for rejecting the $G\lesssim 0$ phenomenological solutions.

V. APPLICATION TO ^{6}Li$(\pi^-,\gamma)_{1s}$ ^{6}He

The radiative capture rate from the 1s atomic orbital is given in the impulse approximation by[11]

$$\Lambda_\gamma(1s)=A^2\frac{k}{m_\pi}\left(1+\frac{m_\pi}{m}\right)^2\left(1+\frac{k}{M}\right)^{-1}\times\frac{(4\pi)^2}{2J_i+1}\,|\phi_\pi(0)|^2\langle M\rangle^2\,, \tag{14}$$

where $\hbar=c=1$, k is the photon momentum in the c.m. system, and m_π, M are the pion and nuclear masses. The constant A is the elementary dipole amplitude $E_{0+}(\pi^-)=(3.26\pm0.04)\times10^{-2}m_\pi^{-1}$ (Ref. 11). The transition matrix element between the states J_i and J_f is

$$\langle M\rangle^2=(4\pi)^{-2}\sum_{M_i M_f\lambda}\int|\langle J_f|e^{-i\vec{k}\cdot\vec{r}}(\vec{\sigma}\cdot\vec{\epsilon}_\lambda)\tau^-|J_i\rangle|^2d\hat{k}\,, \tag{15}$$

where $\vec{\epsilon}_\lambda$ is the photon polarization ($\lambda=\pm1$) and τ^- is the isospin operator defined by $\tau^-|p\rangle=|n\rangle$. The operator notation implies a sum over nucleons. Since the pion wave function varies slowly over the nuclear volume, it has been removed from the nuclear matrix element and replaced by the value

TABLE III. Comparison of the theoretical and phenomenological amplitudes. The results based on the Kuo-Brown two-body matrix elements are indicated by ϵ, the single-particle $p_{1/2}-p_{3/2}$ splitting.

Model	Ground $(1^+, T=0)$ α	β	γ	5.37 MeV $(2^+, T=1)$ G	H	3.56 MeV $(0^+, T=1)$ A	B
$\epsilon=3$ MeV	0.984	0.149	0.010	0.452	0.892	0.960	−0.280
$\epsilon=4$ MeV	0.977	0.205	0.056	0.539	0.843	0.945	−0.328
$\epsilon=5$ MeV	0.966	0.259	0.017	0.597	0.802	0.931	−0.364
Barker	0.992	0.120	−0.028	0.553	0.833	0.934	−0.358
Phen. model	0.979	0.200	0.041	0.460	0.888	0.881	−0.473

at the nuclear center:

$$|\phi_\pi(0)|^2=\frac{R}{\pi}(Z\alpha\mu)^3 . \tag{16}$$

Here, μ is the pion-nuclear reduced mass, and R is a distortion factor which takes into account nuclear size and strong interaction effects. This factor was obtained by computing the pion $1s$ atomic orbital bound by a Gaussian charge distribution ($r_{\rm rms}=2.56$ fm) and modified by a strong potential of the form

$$2\mu V_s(r)=-4\pi(1+m_\pi/m)b_0\rho(r) . \tag{17}$$

Nonlocal and absorptive terms have been ignored in $V_s(r)$, while the isovector (b_1) term vanishes if, as we assume, the proton and neutron distributions are identical. The density $\rho(r)$ was also assumed to be a Gaussian-type distribution.[12] We find

$$R=0.64 \quad \text{for } b_0=-0.030m_\pi^{-1} . \tag{18}$$

The multipole decomposition of Eq. (15) is accomplished by expanding $(\vec\sigma\cdot\vec\epsilon_\lambda)e^{-i\vec k\cdot\vec r}$ in vector spherical harmonics [see e.g., Ref. 13 Eq. (3.30)], and with the Wigner-Eckart theorem one obtains

$$\langle M\rangle^2=\sum_J\left\{|\langle J_f||\vec{\mathrm{M}}_{JJ}\cdot\vec\sigma\tau^-||J_i\rangle|^2+\frac{1}{k^2}|\langle J_f||\vec\nabla\times\vec{\mathrm{M}}_{JJ}\cdot\vec\sigma\tau^-||J_i\rangle|^2\right\} . \tag{19}$$

In the notation of de Forest and Walecka,[13]

$$\vec{\mathrm{M}}^M_{JL}(\vec r)=j_L(kr)\vec{\mathrm{Y}}^M_{JL1}(\Omega) \tag{20}$$

and

$$\frac{1}{k^2}|\langle J_f||\vec\nabla\times\vec{\mathrm{M}}_{JJ}\cdot\vec\sigma\tau^-||J_i\rangle|^2=\left|\left\langle J_f\right|\left|\left[-\left(\frac{J}{2J+1}\right)^{1/2}\vec{\mathrm{M}}_{JJ+1}+\left(\frac{J+1}{2J+1}\right)^{1/2}\vec{\mathrm{M}}_{JJ-1}\right]\cdot\vec\sigma\tau^-\right|\left|J_i\right\rangle\right|^2 . \tag{21}$$

The states J_f in ^{6}He and the $T=1$ levels of ^{6}Li are presumably members of the same isospin multiplet, in which case the matrix elements in Eq. (19) and those for the analog states in ^{6}Li are related by a Clebsch-Gordan coefficient in isospin space. For $T_i=0, T_f=1$ we have

$$|\langle J_f||Q\tau^-||J_i\rangle|^2=2|\langle J_f||\tfrac{1}{2}Q\tau_3||J_i\rangle|^2 , \tag{22}$$

where Q is the appropriate multipole operator. The right side of Eq. (22) was evaluated using the phenomenological ^{6}Li wave functions and transition densities.

The $1s$ radiative capture rates to the ground and first excited states of ^{6}He are summarized in Table IV. The ground state transition rate is in good agreement with the experimental results of Renker *et al.*,[1] but the capture rate to the 1.8 MeV (2^+) state is about 70%, or two standard deviations above the experimental value. For the excited state transition the multipole contributions are estimated to be in the ratio $M1/E2/M3 = 0.095/0.93/1.0$.

TABLE IV. Radiative pion capture rates from the $1s$ atomic orbital of ^{6}Li based on the phenomenological L–S amplitudes and transition densities.

	^{6}Li → ^{6}He (g.s., 0^+)		
β	B	$\langle M\rangle^2$	$\Lambda_\gamma(1s)$ (sec^{-1})
0.200	−0.473	4.77×10^{-2}	1.39×10^{15}
0.369	−0.537	4.48×10^{-2}	1.30×10^{15}
	Exp. value: $(1.39\pm0.16)\times10^{15}$ (Ref. 1)		
	^{6}Li → ^{6}He (1.8 MeV, 2^+)		
β	G	$\langle M\rangle^2$	$\Lambda_\gamma(1s)$ (sec^{-1})
0.200	0.460	1.96×10^{-2}	5.64×10^{14}
0.369	0.360	1.99×10^{-2}	5.70×10^{14}
	Exp. value: $(3.3\pm1.2)\times10^{14}$ (Ref. 1)		

VI. THE ^{6}Li → ^{6}He (1.8 MeV, 2^+) TRANSITION: MODEL INDEPENDENT CONSIDERATIONS

The difference between the predicted and experimental capture rates to the 1.8 MeV (2^+) state of ^{6}He is puzzling in view of the good agreement achieved for the ground state transition. Therefore, we will consider an alternative approach to the former transition, and show under what circumstances the nuclear matrix elements may be obtained directly from the experimental form factor.

In general, transverse form factors have contributions from both the convection and magnetization currents, while only the latter are relevant, via Eq. (22), to the radiative capture process. If the convection terms are negligible at $q=k$, then the electron scattering form factor gives $\langle M\rangle^2$ directly:

$$\langle M\rangle^2=\frac{2}{\pi}(2J_i+1)\frac{Zm}{k\mu_v}F_T^2(k) , \tag{23}$$

where Z is the charge of the target nucleus and the other symbols have their previous meaning.

The 5.37 MeV transverse form factor has $M1$, $E2$, and $M3$ components, and all the amplitudes and transition densities considered here produce a minimum in $F_{M1}^2(q)$ in the region $q \approx 0.7-0.9$ fm^{-1}. (This minimum has also been suggested by others.[6]) Therefore it seems likely that $F_T^2(q)$ is dominated by the $E2$ and $M3$ terms near $q = k = 0.67$ fm^{-1}, the momentum transfer appropriate for capture to ^{6}He (2^+).

In Appendix A we show that the convection current makes no contribution to $M3$ transitions in a $(1p)^n$ space, and in Appendix B we show that the convection contribution to $F_{E2}^2(k)$ is negligible even when the initial and final state radial functions differ slightly providing $F_{C2}^2(k)$ is small. Then, since the $M1$ term is suppressed, the experimental 5.37 MeV form factor provides a *lower* limit for the sum in Eq. (19). From the experimental form factor (renormalized upward by 1.42) and Eq. (23) we obtain

$$\langle M\rangle^2 = 1.89\times 10^{-2}\,, \qquad \Lambda_\gamma(1s) = 5.42\times 10^{14}\ \text{sec}^{-1}\,, \tag{24}$$

which are not appreciably different from the results in Table IV.

Although we have assumed the configuration space is $(1p)^2$ (but not necessarily harmonic oscillator functions), the preceding arguments are a bit more general. The convection current part of $F_{M3}^2(q)$ vanishes if we expand the basis to include any s- or p-orbital components. Similarly, the remarks about $F_{E2}(q)$ are valid for any $E2$ transition that only involves angular momentum recoupling.

VII. PION PHOTOPRODUCTION NEAR THRESHOLD

Our estimate for the ratio of radiative capture rates to the 2^+ and 0^+ states of ^{6}He is larger than the experimental ratio. Since the pion photoproduction cross sections near threshold leading to the same states in ^{6}He depend essentially on the same nuclear matrix elements, evaluated at nearly the same momentum transfer, one would expect a similar behavior for the ratio of photopion cross sections if the source of disagreement lies in the nuclear wave functions. The predicted ^{6}Li(γ,π^+) ^{6}He(0^+) cross section has already been shown to be in reasonable accord with experiment.[4] Unfortunately, the ^{6}Li$\rightarrow{}^6$He(2^+) experimental data are complicated by the underlying $\alpha+2n$ continuum.

The photopion results are usually expressed in terms of the quantities $a(i\rightarrow f)$, defined in Ref. 4, which are proportional to the matrix elements $\langle M\rangle^2$, Eq. (19), at the appropriate momentum transfers (0.72–0.73 fm^{-1}). We will not deal here with the complications introduced by the distorted pion wave functions; this is discussed, for example, in Refs. 7 and 2. Our estimate of the ratio, and the experimental value, are

$$\frac{a[^6\text{Li}\rightarrow{}^6\text{He}(2^+)]}{a[^6\text{Li}\rightarrow{}^6\text{He}(0^+)]} = 0.57 \quad \text{(phen. model)}$$

$$= 0.70\pm 0.24 \quad \text{(expt.; Ref. 4)}.$$

Although well within the quoted error, the theoretical ratio is lower than experiment, in contrast to the radiative capture situation.

Note that the excited state cross section may contain a contribution from the $\alpha+2n$ background, which we have not included in our calculation. This would serve to increase the experimental ratio above the theoretical value.

VIII. DISCUSSION

The ^{6}Li$(2^+, 5.37$ MeV) form factor has been used both directly and indirectly to estimate the RPC rate to ^{6}He(2^+), and the results are consistently about 70% above the experimental value of Renker *et al.*

Since our prediction is relatively model independent, the origin of the discrepancy likely lies elsewhere. Contamination of the experimental cross section by the nearby $\alpha+2n$ continuum is not the problem, since the theoretical value is already too large. It can be argued that we are pushing the model too far in the sense that the $2^+, T=1$ states are not true analogs, that is, they may not have identical radial functions as we assumed in applying Eq. (22). The 2^+ states have different natural widths and dispositions with respect to the two- and three-body thresholds, so some difference in the radial structure is expected, but it would have to be unreasonably large to resolve the discrepancy, and furthermore would destroy the favorable agreement we achieve with the photopion cross sections.

To summarize, the (e,e'), $(\pi^-,\gamma)_{1s}$, and (γ,π^+) cross sections to the $0^+, T=1$ levels are consistent, but a marked disagreement of unknown origin exists among the transitions to the $2^+, T=1$ states.

This work was supported by the Natural Sciences and Engineering Research Council of Canada.

APPENDIX A

In this appendix, we show that in a $(1p)^n$ model space, the convection part of the nuclear transition current density does not contribute to $M3$ transitions.

The $M\lambda$ matrix element is

$$\langle f|T^{\rm mag}_{\lambda\mu}(q)|i\rangle=\int d\vec{r}\,\vec{J}_{fi}\cdot[j_\lambda(qr)\vec{Y}^{\mu}_{\lambda\lambda1}(\Omega)]\,, \quad \text{(A1)}$$

where $\vec{J}_{fi}$ is the transition current density, and here we are concerned only with the convection part of $\vec{J}_{fi}$. In the approximation that $T^{\rm mag}_{\lambda\mu}$ is a one-body operator, Eq. (A1) may be expanded in terms of single-particle matrix elements between states ϕ_i and ϕ_f, where

$$\phi_i=R(r_j)Y_{l_i m_i}(\Omega_j)\quad \phi_f=R'(r_j)Y_{l_f m_f}(\Omega_j)\,. \quad \text{(A2)}$$

The single-particle current, symmetrized to satisfy the continuity equation, is

$$\vec{J}_{fi}(\vec{r}_j)=\left(\frac{-ie_j}{2m}\right)[\phi_f^\dagger\vec{\nabla}\phi_i-(\vec{\nabla}\phi_f)^\dagger\phi_i]\,, \quad \text{(A3)}$$

where $e_j=[1+\tau_3(j)]/2$ is the charge of the particle. For simplicity, the particle label will be suppressed in the following. Combining Eqs. (A3) and (A1), we obtain the general single-particle term

$$\langle R'l_fm_f|T^{\rm mag}_{\lambda\mu}(q)|Rl_im_i\rangle$$

$$=\left(\frac{-ie}{m}\right)\langle R'l_fm_f|j_\lambda(qr)\vec{Y}^{\mu}_{\lambda\lambda1}(\Omega)\cdot\vec{\nabla}|Rl_im_i\rangle\,. \quad \text{(A4)}$$

Using the definition of the vector spherical harmonics,

$$\vec{Y}^{\mu}_{\lambda\lambda1}(\Omega)=\sum_{\nu q}(\lambda\nu1q|\lambda1\lambda\mu)Y_{\lambda\nu}(\Omega)\vec{e}_q \quad \text{(A5)}$$

and the closure property of the spherical harmonics, Eq. (A4) may be written

$$\langle R'l_fm_f|T^{\rm mag}_{\lambda\mu}(q)|Rl_im_i\rangle=\left(\frac{-ie}{m}\right)\sum_{q\nu}\sum_{lm}(\lambda\nu1q|\lambda1\lambda\mu)\langle l_fm_f|Y_{\lambda\nu}(\Omega)|lm\rangle\langle lmR'|j_\lambda(qr)\nabla_q|Rl_im_i\rangle\,. \quad \text{(A6)}$$

The sum over the projections is facilitated by the Wigner-Eckart theorem, giving

$$\langle R'l_fm_f|T^{\rm mag}_{\lambda\mu}(q)|Rl_im_i\rangle=\left(\frac{-ie}{m}\right)(-1)^{l_f-m_f}(2\lambda+1)^{1/2}\sum_l\begin{pmatrix}l_f&\lambda&l_i\\ m_f&-\mu&-m_i\end{pmatrix}\begin{Bmatrix}l_f&\lambda&l_i\\1&l&\lambda\end{Bmatrix}\langle l_f||Y_\lambda||l\rangle$$

$$\times\langle R'l||j_\lambda(qr)\vec{\nabla}||Rl_i\rangle\,, \quad \text{(A7)}$$

which vanishes if $\lambda>l_i+l_f$. In other words, the convection part of $T^{\rm mag}_{\lambda\mu}$ is a tensor operator of rank λ in the orbital angular momentum space. Thus, the convection current does not contribute to the $M3$ transition in a model space restricted to s- and p-wave orbitals.

APPENDIX B

We wish to show that the convection current makes a negligible contribution to the 5.37 MeV transverse $E2$ form factor at momentum transfers corresponding to the radiative pion capture, $q\approx0.67$ fm^{-1}. Actually, the argument is more general and applies to any $E2$ form factor involving recoupling within a $(1p)^n$ configuration, if the longitudinal ($C2$) form factor is known to be small.

The $E\lambda$ matrix element is

$$\langle f|T^{\rm el}_{\lambda\mu}(q)|i\rangle=\frac{1}{q}\int d\vec{r}\,\vec{J}_{fi}\cdot\vec{\nabla}\times[j_\lambda(qr)\vec{Y}^{\mu}_{\lambda\lambda1}(\Omega)]\,, \quad \text{(B1)}$$

where as before we retain only the convection part of $\vec{J}_{fi}$. Using various integral identities and the continuity equation, Eq. (B1) becomes

$$\langle f|T^{\rm el}_{\lambda\mu}(q)|i\rangle=-\left(\frac{\omega_{fi}}{q}\right)\left(\frac{\lambda+1}{\lambda}\right)^{1/2}$$

$$\times\int d\vec{r}\,\rho_{fi}Y_{\lambda\mu}(\Omega)\left[j_\lambda(qr)-\left(\frac{qr}{\lambda+1}\right)j_{\lambda+1}(qr)\right]$$

$$+\frac{iq}{[\lambda(\lambda+1)]^{1/2}}\int d\vec{r}\,M_{\lambda\mu}\vec{r}\cdot\vec{J}_{fi}\,, \quad \text{(B2)}$$

where ρ_{fi} is the transition charge density, $\omega_{fi}=E_f-E_i$ is the excitation energy, and

$$M_{\lambda\mu}=j_\lambda(qr)Y_{\lambda\mu}(\Omega)\,. \quad \text{(B3)}$$

The first term in Eq. (B2), without the $j_{\lambda+1}(qr)$ part, is the longitudinal (Coulomb) matrix element reduced by the factor $(-\omega_{fi}/q)[(\lambda+1)/\lambda]^{1/2}$, which is much less than unity. For $E2$ transitions in a harmonic oscillator $(1p)^n$ configuration, the $j_{\lambda+1}(qr)$ part reduces the first term even further providing $(qb_0)^2/6<1$, and this is satisfied for $q\doteq0.67$ fm^{-1}. Finally, we have shown that $F_L{}^2(q)<2\times10^{-4}$ for the 5.37 MeV state, so the contribution of the first term in Eq. (B2) to $F_{E2}{}^2(q)$ is less than 5×10^{-7} and completely negligible. Therefore, we have

$$\langle f|T^{\mathrm{el}}_{\lambda\mu}(q)|i\rangle \approx \frac{iq}{[\lambda(\lambda+1)]^{1/2}}\int d\vec{r}\, M_{\lambda\mu}\,\vec{r}\cdot\vec{J}_{fi}\,. \quad \text{(B4)}$$

Combining Eqs. (A3) and (B4), we obtain the single-particle matrix element

$$\langle R'l_f m_f|T^{\mathrm{el}}_{\lambda\mu}(q)|Rl_i m_i\rangle \approx \left(\frac{q}{2m}\right)\frac{e}{[\lambda(\lambda+1)]^{1/2}}\int d\vec{r}\, M_{\lambda\mu} r\left(\phi_f^\dagger\frac{\partial\phi_i}{\partial r}-\frac{\partial\phi_f^\dagger}{\partial r}\phi_i\right). \quad \text{(B5)}$$

For transitions involving angular momentum recoupling within the $1p$ shell, Eq. (B5) vanishes if ϕ_i and ϕ_f have identical radial functions, such as in the usual harmonic oscillator model. We may obtain an order of magnitude estimate of the form factor when the radial functions are not the same, by considering oscillator functions with different oscillator parameters in the initial and final $1p$ orbitals. If b_0 and b_0' are, respectively, the initial and final oscillator parameters, the convection current part of the $E2$ form factor which follows from Eq. (B5), relative to the total longitudinal $C2$ form factor, is given by

$$\frac{F^{\mathrm{conv}}_{E2}(q)}{F_{C2}(q)}=\left(\frac{49}{6}\right)^{1/2}\left(\frac{q}{2m}\right)\left(\frac{1-\eta^2}{1+\eta^2}\right)\left(1-\tfrac{2}{7}y\right), \quad \text{(B6)}$$

where $\eta = b_0'/b_0$ and

$$y=\frac{2\eta^2}{1+\eta^2}\left(\frac{qb_0}{2}\right)^2. \quad \text{(B7)}$$

(This expression is independent of the j-j configuration amplitudes.) Then, with $q = 0.67$ fm^{-1}, $\eta = 1.2$ and $F_{C2}^2(q) < 2\times10^{-4}$, Eq. (B6) yields $|F^{\mathrm{conv}}_{E2}(q)|^2 < 3\times10^{-7}$. This is the same order as the result generated by the first term of Eq. (B2), and even if both contributions add constructively, the total form factor (squared) is 2×10^{-6} and therefore negligible.

[1] D. Renker *et al.*, Phys. Rev. Lett. 41, 1279 (1978).
[2] J. C. Bergstrom, I. P. Auer, and R. S. Hicks, Nucl. Phys. A251, 401 (1975).
[3] J. C. Bergstrom, U. Deutschmann, and R. Neuhausen, Nucl. Phys. A327, 439 (1979).
[4] G. Audit *et al.*, Phys. Rev. C 15, 1415 (1977).
[5] F. Eigenbrod, Z. Phys. 228, 337 (1969).
[6] R. Neuhausen and R. M. Hutcheon, Nucl. Phys. A164, 497 (1971).
[7] J. B. Cammarata and T. W. Donnelly, Nucl. Phys. A267, 365 (1976).
[8] L. W. Fagg, R. A. Lindgren, W. L. Bendel, and E. C. Jones, Jr., Phys. Rev. C 15, 1181 (1977).
[9] F. Ajzenberg-Selove and T. Lauritsen, Nucl. Phys. A227, 1 (1974).
[10] F. C. Barker, Nucl. Phys. 83, 418 (1966).
[11] H. W. Baer, K. M. Crowe, and P. Truöl, Adv. Nucl. Phys. 9, 177 (1977).
[12] G. C. Li, I. Sick, R. R. Whitney, and M. R. Yearian, Nucl. Phys. A162, 583 (1971).
[13] T. deForest, Jr. and J. D. Walecka, Adv. Phys. 15, 1 (1966).